Chemistry International 7(2) (2021) 79-89

International Scientific Organization
http://iscientific.org/
Chemistry International
www.bosaljournals.com/chemint/

# Adsorption of crystal violet dye onto olive leaves powder: Equilibrium and kinetic studies

**Khaled Muftah Elsherif[1,*], Abdelmeneim El-Dali[1], Asma Amar Alkarewi[2], Abdunaser Mabrok Ewlad-Ahmed[2] and Abdullah Treban[2]**

[1]Chemistry Department, Faculty of Science, University of Benghazi, Benghazi, Libya
[2]Chemistry Department, Faculty of Arts and Science Msallata, Elmergib University, Al-Khoms, Libya
*Corresponding author's E. mail: Elsherif27@yahoo.com

**A R T I C L E I N F O**

**Article type:**
Research article
**Article history:**
Received August 2020
Accepted November 2020
April 2021 Issue
**Keywords:**
Biosorption
Olive leaves
Crystal violet
Isotherms model
Kinetic study

**A B S T R A C T**

Adsorption of crystal violet dye from aqueous solutions applying olive leaves powder (OLP) as a biosorbent has been examined under various experimental circumstances. The influence of contact time, pH, initial concentration of studied dye and adsorbent dose on the adsorption process has been investigated applying batch experiments. The concentration of remaining dye has been determined using molecular absorption spectrometry at wave length of 580 nm. The maximum removal of studied dye has been realized at pH 7.5 with a percent removal of 99.2% after 20 min of agitation time. Langmuir, Freundlich, and Temkin isotherm models exemplify the best fit for the experimental data; while the elevated adsorption capacity was 181.1 mg.g$^{1}$. Adsorption kinetics of crystal violet was expected sufficiently with the empirical pseudo-second-order model. Corresponding to the adsorption capacity, olive leaves powder thought as a low cost, effective, and environmentally friendly biosorbent for the removal of crystal violet dye from aqueous solutions.



**Capsule Summary:** Olive leaves powder has a substantially larger capacity to remove the crystal violet dye. It showed the highest removal values in basic medium. It is an effective, low cost, and environmentally friendly adsorbent.

**Cite This Article As:** K. M. Elsherif, A. El-Dali, A. A. Alkarewi, A. M. Ewlad-Ahmed and A. Treban. Adsorption of crystal violet dye onto olive leaves powder: Equilibrium and kinetic studies. Chemistry International 7(2) (2021) 79-89.
https://doi.org/10.5281/zenodo.4441851

## INTRODUCTION

The ionic and cationic dyes synthesis plays a vital role in the chemical industries, i.e., textile and leather, as well as in the food and paper industries. Commercial dyes are used in large quantities, producing more than eight thousand tons annually, half or more of which are azo dyes (Mahmood et al., 2018; Nworie et al., 2019). Waste of these dyes is deposited in water bodies, which causes concern for the environmental problems. Textile dyes are often complex organic molecules, which are usually challenging to be biologically broken down. They are to be attached to the fabric fiber to confer color to them. If these more commonly organic compounds are discharged into water bodies, they may mean real sources of pollution. Due to their recalcitrant nature, they impart long term color to the aqueous industrial effluent and reduce the penetration of sunlight, which compromises the aquatic life (Araújo et al., 2006; Caldeira et al., 2018). Dyes are of a harmful and chromogenic nature, which has made the attention of researchers in the industry recently a focus on how to dispose of industrial and waste related to dyes

entirely. Various methods have been applied to remove dyes and include chemical coagulation, oxidation, flocculation, ozonation, biological process, membrane-based separation method, photocatalytic process, and sonochemical process electrochemical process and adsorption [El-Hashani et al., 2018a; Elsherif et al., 2017a; 2017b; 2014a; 2014b; Elsherif and Yaghi, 2017a; 2017b; 2016; Okareh and Adeolu, 2013). Researchers' comparison of the purposes for dye removal implicated adsorption as the most efficient, effective and green method (Petrovic et al., 2011). Similarly, activated carbon has shown promising outcomes and extensively studied among the sorbents, but its high cost is a substantial limitation to researchers prompting a search for an alternative low-cost sorbent of equivalent effectiveness, efficiency, and environmentally benign (Nworie et al., 2019).

The effluent is treated using adsorption process, as one of the most probable ways to treat effluents consists of a physical or chemical reaction between the surface of the porous solid and the components of the particles from the liquid phase (Gupta, 2009). The adsorption process is mainly governed by solid-state properties, such as the surface area, density, pore size and moisture, and the liquid material, such as absorption, solubility, polarity, and particle size. Also, through some conditions such as temperature, pH of the medium and the nature of the solvent (Caldeira et al., 2018). A biosorbent is defined as an adsorbent which consists of biomass. Low-cost and safe wastewater treatment with biological absorption makes it a practical and popular method for many other treatment options available (Reddy et al., 2015; Zaidan et al., 2013). Because the adsorbent preparation from biomass is inexpensive in moderation and the adsorbent generated can be reused in many cases. Biological absorption is an uncomplicated and highly efficient method of removing pollutants from the water, compared to many other wastewater treatment options. Biological absorption results in less waste and less use of chemicals than chemical treatment, which reduces the chances of environmental pollution caused by chemicals (Alkherraz et al., 2020a; 2020b; 2019; Fosso-Kankeu et al., 2019; Zaidan et al., 2013).

The purpose of this study was to investigate the effectiveness of olive leaves powder (OLP) to adsorb crystal violet from the aqueous solution. The effect of contact time, pH, concentration, and adsorbent mass on the removal efficiency was studied under continuous stirring. The results were modeled with different isotherms and kinetic models.

## MATERIAL AND METHODS

### Chemical and Reagents

Crystal violet (99%) from WinLab-UK, HCl (37%) from Merck, NaOH (99%) from Analar were utilized in this work. The chemical structure and the solution of crystal violet are shown in figure 1. De-ionized water was used to prepare all the solutions. First, a 1000 ppm crystal violet was prepared as stock solution in de-ionized water and then working solutions of required concentrations were made by suitable dilution. Solutions of 0.1 M HCl and 0.1 M NaOH were used to adjust the pH.

### Preparation of biosorbent

Fresh olive leaves were gathered from Misallta area in west Libya, washed with distilled water several times to eliminate all the contaminants such as small insects, dust, and other foreign body. Olive leaves were then dried in an oven at about 60°C for 24 h. The olive leaves were ground using a laboratory mill. Finally, grinded olive leaves were then sieved through 125 µm size fraction using an American Society for Testing and Materials (ASTM) standard sieve. The reason of drying the washed olive leaves is to remove all the volatile components and moisture content that could exist in the biosorbent.

### Adsorption process

Adsorption was carried out by shaking 0.1 g of biosorbent with a speed of 150 rpm with 50 ml of 50 ppm crystal violet solution within the required time. The speed of agitation is kept constant for each cycle during the experiment to guarantee equal mixing. The solutions were then filtered by means of filter paper, and the filtrate was analyzed using UV-VIS spectrophotometer at a wavelength of 580 nm to determine the concentration in the solution. This process was repeated to study various parameters (contact time, pH, dye concentration, and adsorbent dose). For contact times ranging from 5 min to 70 min, the same adsorption procedure was repeated using 0.1 g biosorbent dose, in 50 ml solution, and using 50 ppm concentration of crystal violet. To study the effect of pH, various solutions with different pH values (2-11) and the same concentration (50 ppm) were used. The effect of adsorbent dose was carried out using 50 ppm concentration of crystal violet at the optimum pH and contact time (determined before) and varying the biosorbent dose from 0.01 to 0.14 g. The effect of initial crystal violet concentration was studied using different concentrations of crystal violet ranging from 10 to 100 ppm. Every other parameters were kept constant at the optimum in each experiment when the parameter of interest was investigated.
The adsorption capacity, $Q_e$ (mg/g) and percentage removal % R of crystal violet onto the OLP were calculated by the following equations 1-2 (El-Hashani et al., 2018b; Elsherif et al., 2018a):

$$Q_e = \frac{(C_0 - C_e) \times V}{W} \quad (1)$$

$$\% R = \frac{C_o - C_e}{C_o} \times 100 \quad (2)$$

Where: where $C_o$ (mg/L) is the initial crystal violet concentrations, $C_e$ (mg/L) is the crystal violet concentrations at equilibrium, V (L) is the volume of crystal violet solution, and W (g) is the weight of the biosorbent.

**Table 1:** Langmuir, Freundlich, D-R and Temkin isotherm constants for adsorption of crystal violet onto OLP

| Isotherms | Parameters | | |
|---|---|---|---|
| Langmuir | $q_m$ | b | $R^2$ |
| | 133.33 | 0.042 | 0.964 |
| Freundlich | $K_f$ | n | $R^2$ |
| | 5.54 | 1.12 | 0.955 |
| Temkin | β | A | $R^2$ |
| | 35.74 | 1.20 | 0.932 |
| Dubinin-Radushkevich | $q_m$ | β | $R^2$ |
| | 29.01 | $1.0x10^{-6}$ | 0.7686 |

**Table 2:** Kinetic parameters of crystal violet adsorption onto OLP

| Models | Parameter | | |
|---|---|---|---|
| First Order | $Q_e$ (mg/g) | $k_1$(1/min) | $R^2$ |
| | 32.98 | $7.0x10^{-5}$ | 0.3603 |
| Second Order | $Q_e$ (mg/g) | $k_2$ (g/mg.min) | $R^2$ |
| | 12.32 | 0.63 | 1.000 |

**Analysis**

Spectrophotometric determination was accomplished through 6305 UV-VIS Spectrophotometer from JENWAY. The pH of the solution was determined with 3505 pH Meter from JENWAY.

**RESULTS AND DISCUSSION**

By UV-VIS. Spectrophotometer, the concentrations of crystal violet dye in the solutions were determined. The range of calibration curve of dye prepared from the stock solution varies between 2-8 ppm, as shown in Figure 2. The crystal violet dye response was found to be linear in the investigation concentration range at $\lambda_{max}$ = 580 nm (determined from figure 3), and the linear regression equation was y = 0.1992x with a high correlation coefficient ($R^2$= 0.996). The concentrations of crystal violet in the solutions before and after equilibrium adsorption were determined from the calibration curve.

**Effect of pH on adsorption**

One of the most significant factors that influence the adsorption potential of biosorbent is its pH (Betiku and Sheriff, 2014; Elsherif et al., 2018b; Nworie et al., 2019). Many characteristics of biosorbent that influence its capability to capture particulates such as the extent of ionization of solution adsorbate, charge on the sorbent surface and sorbent functional groups resident on the reactive sites (Uchimiya et al., 2011). pH effect on the adsorption of crystal violet onto OLP was investigated by varying the pH between 2-11 at 298 K for 20 min and the result shown in Figure 4. The highest percentage of the cationic dye crystal violet adsorbed representing the maximum adsorption capacity was 87.06 % at pH 7.5, and the lowest percentage was 62.63 % at pH 2. Above pH 8, the adsorption remained reasonably constant. This observation is consistent with the study by (Nasuna et al., 2010) on adsorption of Methylene Blue onto lignocellulosic wastes. The adsorption was observed to be low at acidic pH values against the basic pH regions found in other studies (Nworie et al., 2019), probably because of the decreased electrostatic forces of interaction between OLP's surface, which is positively charged and the cationic crystal violet. The percentage reduction of adsorption infers competition between the similar charges on both surfaces of adsorbent and sorbate. As pH increased from 5 and above, the negative charges on OLP increased due to an increase in negative sites. This led to increased adsorption as the electrostatic attraction was increased, and $OH^-$ presence at the basic region encouraged adsorption. The equilibrium shift as observed could be associated with adsorbent surface functional group dissociation and alteration on adsorption (Singh et al., 2011). More significant removal of crystal violet was observed at basic pH. There is a decrease in the number of positive sites and an increase in negative charges at the basic pH region.

**Effect of initial dye concentration and contact time**

The initial concentration of adsorption is an essential characteristic of the adsorption study (Elsherif et al., 2019). The effect of the initial concentration of crystal violet on the adsorption capacity of OLP was investigated by varying the initial concentration from 10 ppm to 100 ppm. Results in Figure 5 exhibit the amount of crystal violet adsorbed increases with increasing concentration.

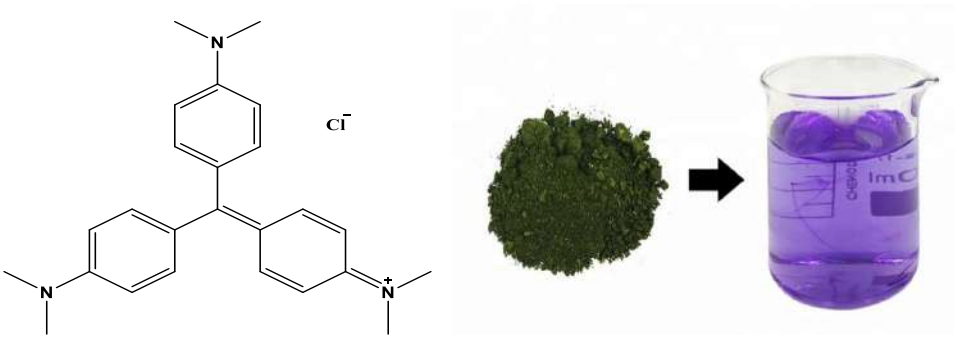


**Fig. 1:** Chemical structure and solution of Crystal Violet dye

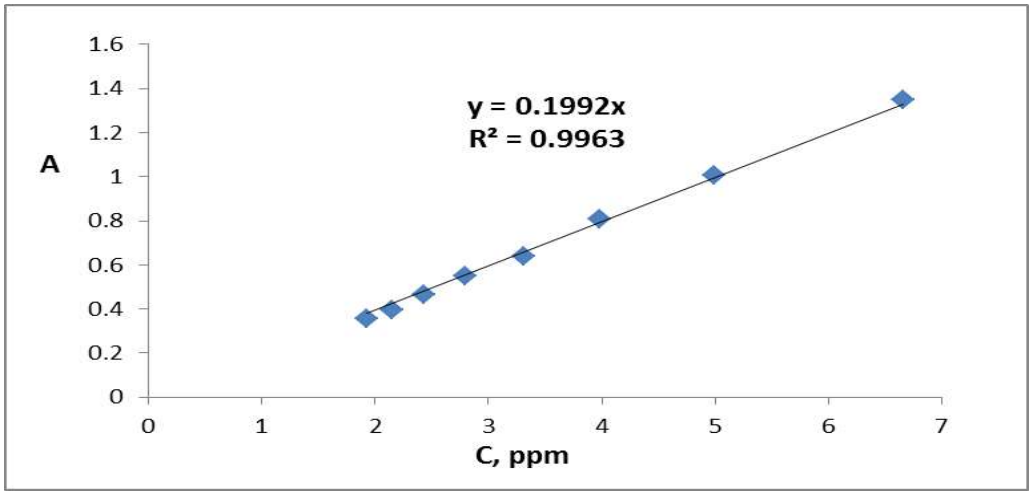


**Fig. 2:** Calibration curve of crystal violet at 580 nm (A = absorbance)

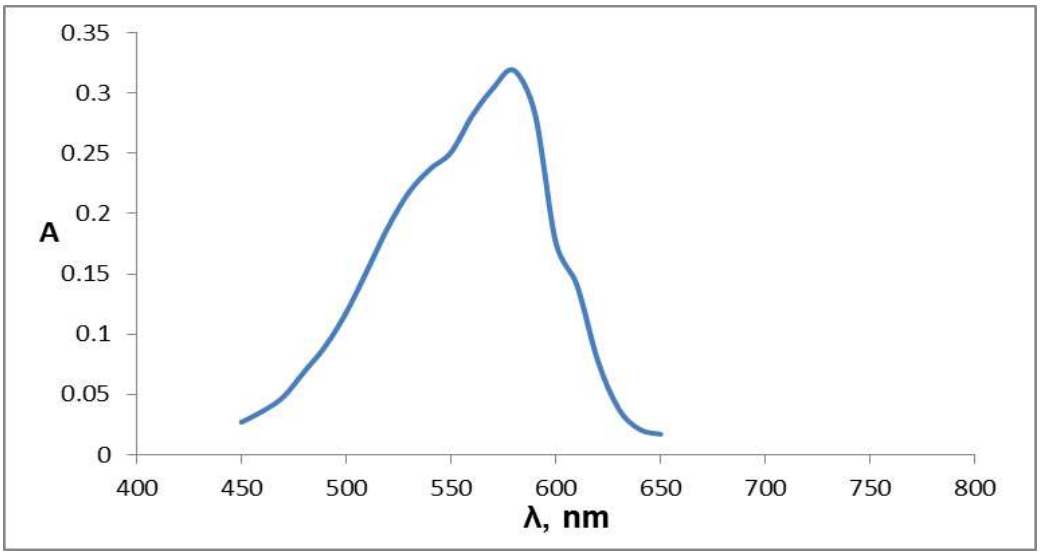


**Fig. 3:** Absorption spectrum of crystal violet (A = absorbance)

This observation is consistent with the studies (El-Hashani et al., 2018b) on the removal of Eriochrome Black T by waste tea powder. Sorption capacity increased as the initial crystal violet concentration increased from 10 ppm to 100 ppm, and equilibrium was attained, indicating increased fractional crystal violet adsorption. The transport of crystal violet molecules to interior regions of OLP controls the adsorption process, and liquid film diffusion and intra-particle diffusion mechanisms could be responsible as recognized in kinetics investigations.. The variation of crystal violet adsorbed versus contact time is shown in Figure 6. As the contact time increased, the adsorption increased until it reached an equilibrium state at 20 minutes. The adsorbent surface performs fast adsorption protection in the initial period, with a gradual decrease in the adsorption speed due to the blockage of the adsorption sites. The decline continues until it reaches an equilibrium state. The removal of violet crystals in the initial period was rapid in the initial period, then the adsorption speed decreases when approaching equilibrium. This phenomenon explains that adsorption sites are initially active sites but are gradually filled with time, which leads to blockage of absorption sites and a noticeable decrease or lack of availability of the free site. This observation is in agreement with the studies (El-Hashani et al., 2018b; Elsherif et al., 2018a; 2018b; 2017a; 2017b) on the removal of heavy metals from agricultural waste biosorbents.

**Effect of adsorbent dosage**

The effect of adsorbent dosage on the removal of crystal violet was studied by varying the dosage of adsorbent from 0.2 to 2.8 g/L at optimum pH (7.5) and dye concentration 50 ppm. Figure 7 shows that the dosage of adsorbent significantly influences the amount of crystal violet adsorbed. Increasing the amount of adsorbents from 0.2 to 2.8 g/L led to a decrease in adsorbent capacity because with increasing adsorbent dose, unsaturated residual adsorption sites reduce adsorption capacity during the adsorption process (Calvete et al., 2010). The results of studies conducted by Seid Mohammadi et al. (2015) and Gupta et al. (2014) are consistent with our results (Gupta et al., 2014; Seid mohammadi et al., 2015).

**Equilibrium modeling**

***Langmuir isotherm***

Adsorption is a homogeneous process. It inculcates one layer without adsorption covered in the surface of the absorbent plane that is transported due to uniform energy as shown in Eq. 3 (Mahmood et al., 2018).

$$q_e = \frac{Q_m b C_e}{1+bC_e} \quad (3)$$

Where, $Q_m$ is maximum adsorption capacity (mg/g), b the Langmuir constant related to free interaction binding energies of the adsorption (L/mg), $q_e$ the quantity of dye adsorbed per specific unit mass of adsorbent (mg/g), and $C_e$ the equilibrium solute concentration (mg/L). The reversibility of the adsorption and presence of adsorption sites of fixed numbers describes the nature of the model. Linear form of the Langmuir model is shown in Eq. 4 (Banerjee and Chattopadyaya, 2017).

$$\frac{1}{q_e} = \frac{1}{Q_m} + \frac{1}{bQ_m C_e} \quad (4)$$

Simulated data were used in the plot of $1/q_e$ versus $1/C_e$ by Langmuir equation. Figure 8 indicates a very high sorption constant for OLP (326.79 mmolkg$^{-1}$), with a high correlation coefficient ($R^2$) of 0.964 and which was in the range of commercially available activated carbons (101.395 mmolkg$^{-1}$) and other biosorbents (11.680 mmolkg$^{-1}$) (Dada et al., 2013). The results obtained from Langmuir model are shown in Table 1.

The dimensionless separation factor $R_L$ is a measure of the desirability and favorability of the model and the Langmuir parameter b (Langmuir isotherm model constant) was evaluated using Hall relation (Eq. 5) (Banerjee and Chattopadyaya, 2017; Mahmood et al., 2018).

$$R_L = \frac{1}{1+bC_o} \quad (5)$$

Where, $C_o$ is the initial dye concentration. The value of $R_L$ is essentially important and defines the isotherm to be linear ($R_L$ = 1), unfavorable ($R_L$ > 1) and favorable (0 < $R_L$ < 1) (Banerjee et al., 2017). The study indicated $R_L$ value of 0.32 a confirmation that the adsorption of crystal violet onto OLP was favorable.

***Freundlich isotherm***

Freundlich adsorption occurs in a heterogeneous, multilayer surface where it is considered an ideal model of adsorption. The adsorption process occurs on an unlimited degree of adsorption sites, and the energies exponentially or non-uniformly distributed Freundlich isotherm is expressed in Eq. 6 (Nworie et al., 2019).

$$q_e = K_F C_e^{\frac{1}{2}} \quad (6)$$

The linear form of Freundlich model is shown in Eq. 7.

$$\log q_e = \frac{1}{n} \log C_e + \log K_F \quad (7)$$

Where, n: is the adsorption intensity representing the favorability of the process and measures the degree at which the model deviates from linearity and $K_f$ is the adsorption capacity representing the adsorptive bond strength obtained as the slope and intercept respectively and shown as the linear plot of log $q_e$ against log $C_e$ illustrated in Figure 9.

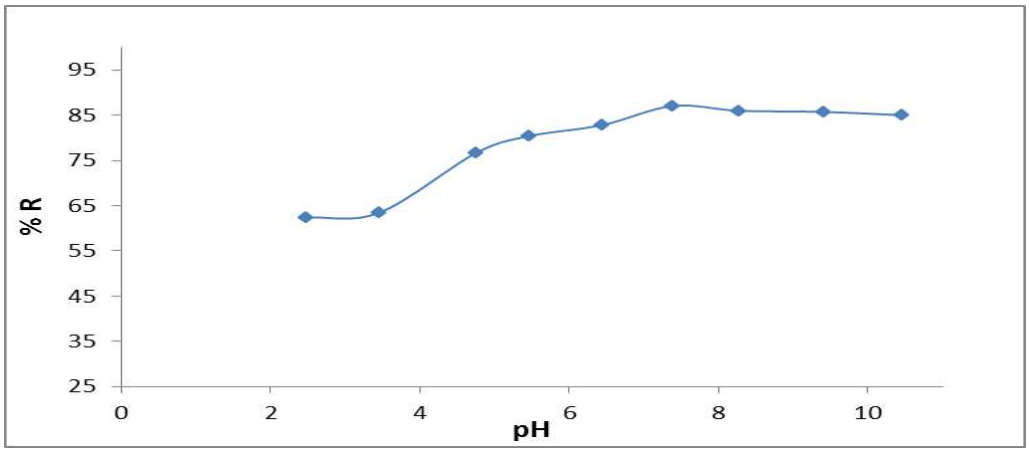


**Fig. 4:** Effect of pH on the adsorption of crystal violet

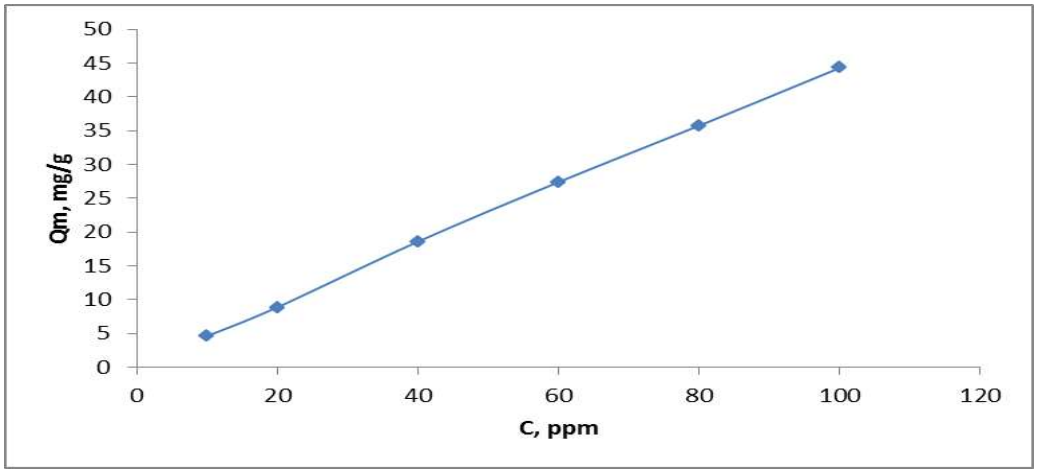


**Fig. 5:** Effect of initial crystal violet concentration on the adsorption onto OLP

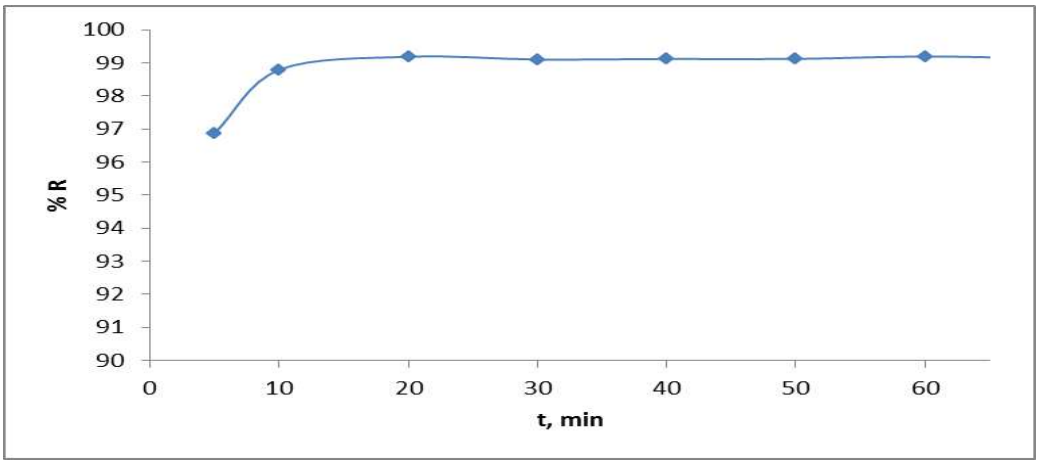


**Fig. 6:** Effect of contact time on the adsorption of crystal violet onto OLP

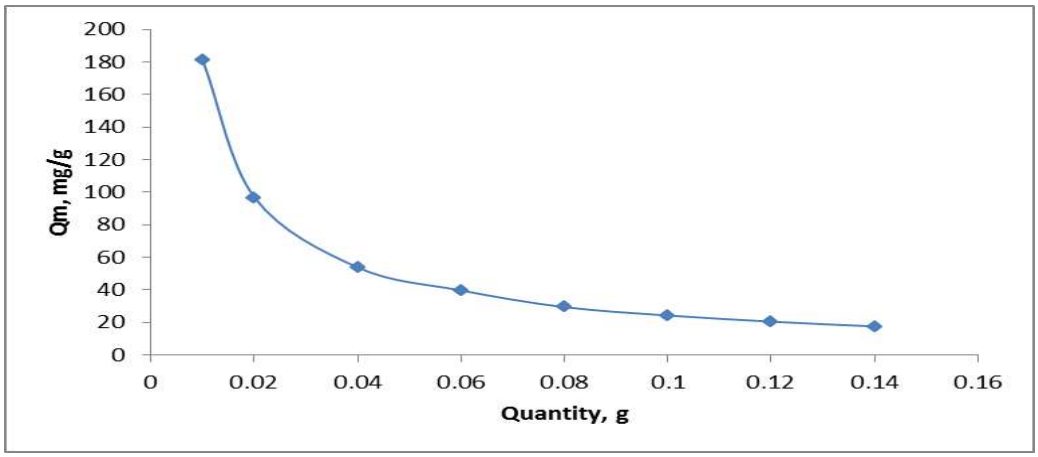


**Fig. 7:** Effect of adsorbent dosage on the adsorption of crystal violet onto OLP

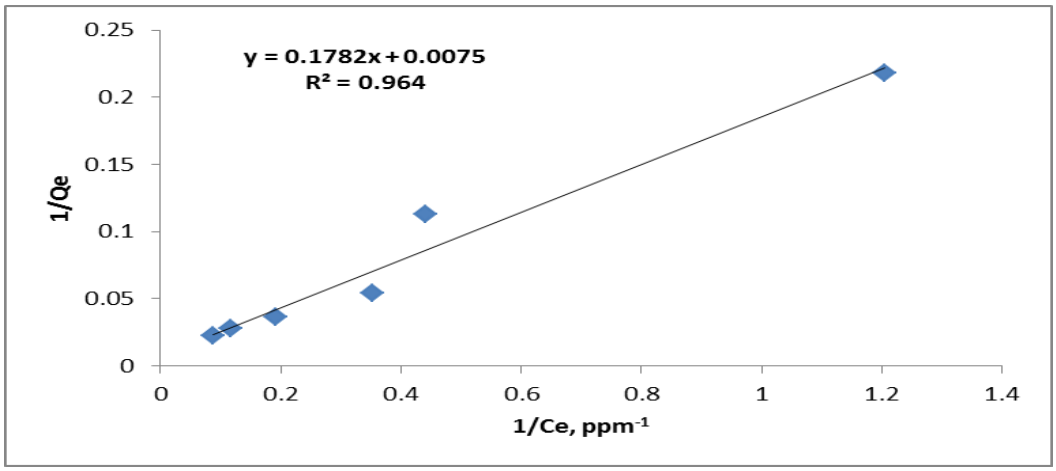


**Fig. 8:** Langmuir isotherm model for the adsorption of crystal violet onto OLP

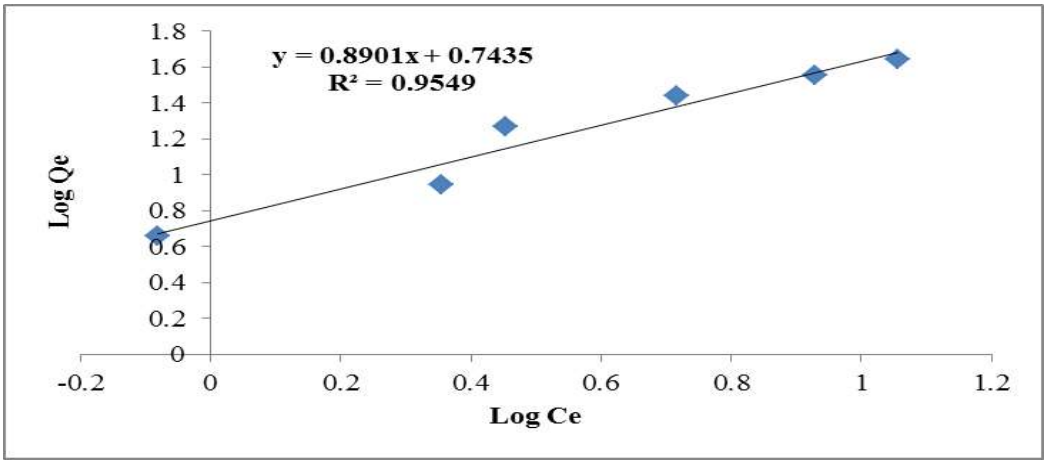


**Fig. 9:** Freundlich isotherm model for the adsorption of crystal violet onto OLP

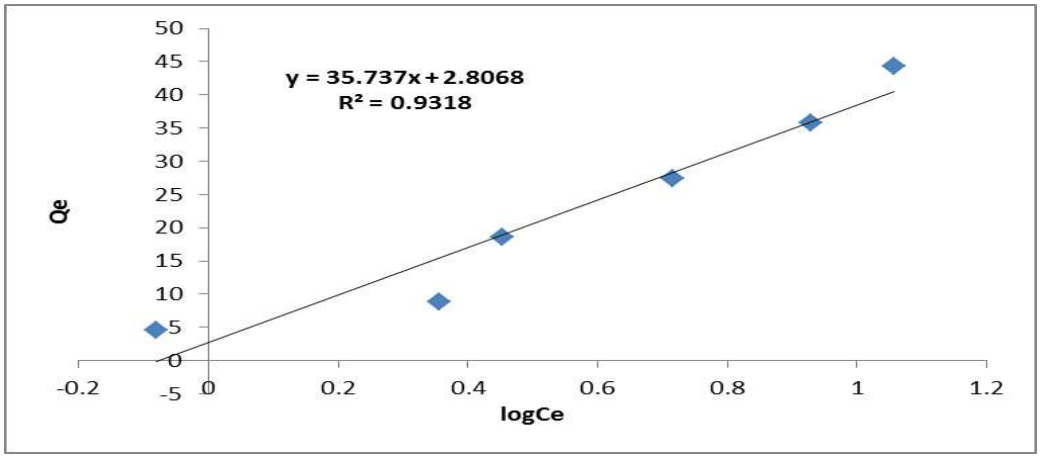


**Fig. 10:** Temkin isotherm plot for the adsorption of crystal violet onto OLP

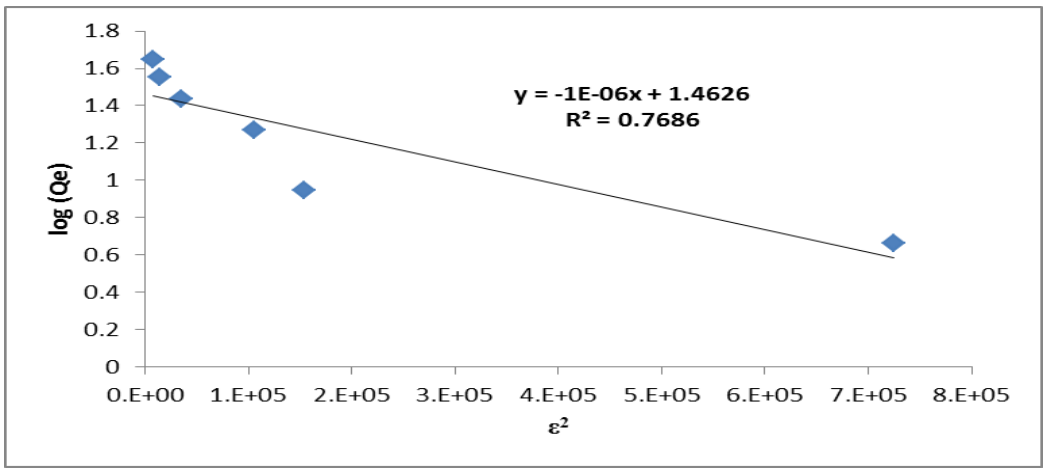


**Fig. 11:** Dubinin-Kaganer-Radushkevich isotherm plot for the adsorption of crystal violet onto OLP

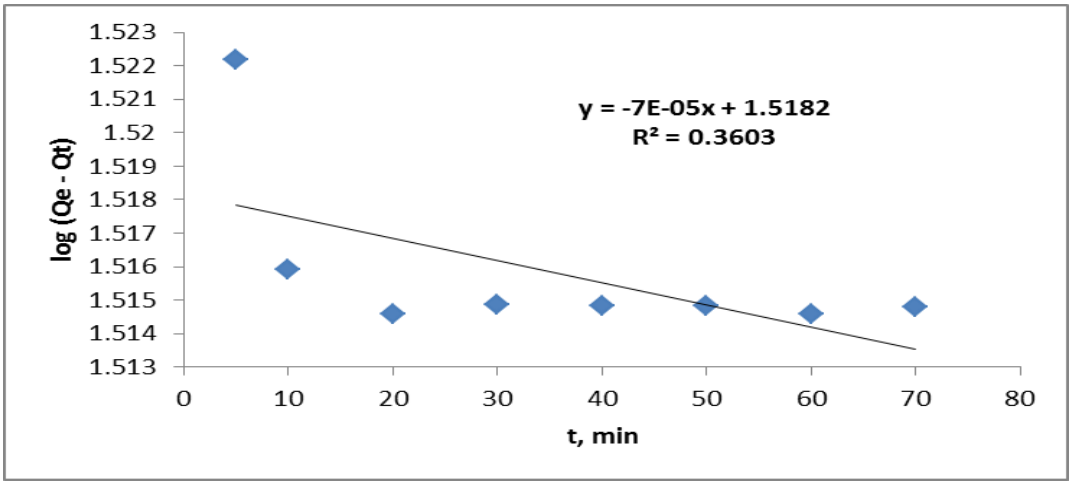


**Fig. 12:** Pseudo-first–order kinetic plot for the adsorption of crystal violet onto OLP

Results show acceptable linearity straight line. Value of n parameter is 1.12 for crystal violet–OLP, suggesting value of 1/n comprised between 0 and 1, indicating a favorable adsorption of crystal violet dye onto OLP. The value of the correlation coefficient was high 0.9549 and comparable with that of Langmuir. The values of n and $K_f$ are presented in Table 1 and show that the Freundlich adsorption process can simulate it since the value of n is more than one (Mahmood et al., 2018).

***Temkin isotherm***

This model, which is co-operatively applied under the condition of an intermediate mode of sorbate concentration, Considers the fall in the heat of the sorption of molecules in the layer to decrease linearly with the area of coverage owing to sorbent or sorbate interaction instead of logarithmic (Banerjee and Chattopadyaya, 2017). The linear form of the Temkin isotherm model is shown in Eq. 7 (Elsherif et al., 2018a).

$$q_e = \beta \log A + \beta \log C_e \quad (7)$$

Where, β is related to the heat of adsorption, and A is the equilibrium binding constant. The plot of $q_e$ against log $C_e$ (Figure 10) gives the slope and intercept as β and A respectively. The values of $R^2$ and the constants are presented in Table 1. The high value of $R^2$ (0.9318) suggests that the model satisfy the experimental data, and similar results was obtained in the adsorption of methylene blue with Activated Rice Husk Biochar (Nworie et al., 2019).

***Durbinin-Kaganer Radushkevich (DKR) isotherm***

Pore filling applied to intermediate concentration range of adsorption with multiple layers is performed using a semi-experimental DKR equation, van der Waals and heterogeneous surface interaction taking into account subsequent Gaussian free energy (Prakash et al., 2014). The linear form of the temperature-dependent model is shown in equation (8) (Elsherif et al., 2018a).

$$\log q_e = \log q_m - \beta \varepsilon^2 \quad (8)$$

The plot of log $q_e$ versus $\varepsilon^2$ represented in Figure 11. The parameter ε regarded as polanyi potential is represented in equation 9 and mean adsorption energy E (KJ/mol) was evaluated using Eq. 10 (Elsherif et al., 2018a).

$$\varepsilon = RT\, log\left[1 + \frac{1}{C_e}\right] \quad (9)$$

$$E = \frac{1}{\sqrt{-2\beta}} \quad (10)$$

Where, ß is DKR constant representing low adsorption energy ($mol^2/KJ^2$), R the molar gas constant (8.314 J $mol^{-1}K^{-1}$), $q_m$ the DKR monolayer adsorption capacity (mg/g), T the absolute temperature (K). The value of E describes the nature of adsorption either as physical or chemical or ion exchange if the value is less than 8 KJ/mol or within 8-16 KJ/mol, respectively (Mahmood et al., 2018). In the present study, the adsorption energy E is 0.707 KJ/mol, which is less than 8 KJ/mol indicating that at the temperature of 298 K in which the adsorption was performed, physical processes are predominant and mainly in operation. From Table 1, the correlation coefficient $R^2$ was low and lower than the other models (0.7686), indicating that the model did not simulate the data well as the other isotherm models.

**Kinetics studies**

Adsorption of adsorbate from solution applied to Lagergren pseudo-first order rate Eq. 11 (Petrovic et al., 2011).

$$\log(q_e - q_t) = \log q_e - \left(\frac{K_1}{2.303}\right) t \quad (11)$$

The linear form of the pseudo-first order kinetic model is shown in Eq. 12 (Nworie et al., 2019).

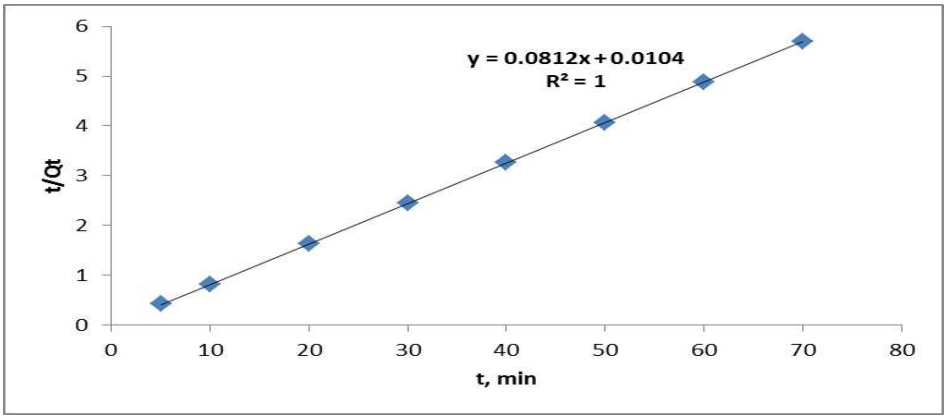


**Fig. 13:** Pseudo-second–order kinetic plot for the adsorption of crystal violet onto OLP

$$log(q_e - q_t) = \log q_e - K_1 t \quad (12)$$

Where, t is the time of contact (min), qt is the quantity of crystal vilet dye at time t, $q_e$ is the quantity of dye adsorbed at equilibrium (mg/g), and $K_1$ pseudo-first-order rate constant. As shown in Table 2 and linear plots in Figure 12, the data have low regression coefficient ($R^2$) of 0.3606 and low value of $K_1$ as 7.0 x $10^{-5}$ $min^{-1}$ and as such the further discussion on the model and the figure was suspended.

The assumption in pseudo-second-order kinetic model is that chemisorption dictates the rate controlling step as illustrated in Eq. 13 (Demirbas, 2004).

$$\frac{t}{q_t} = \frac{1}{K_2 q_e^2} + \frac{t}{q_e} \quad (13)$$

Where, $K_2$ is the second-order rate constant (g/mg.min) and $q_e$ adsorption capacity at equilibrium evaluated as intercept and slope of the linear plot of $t/q_t$ versus t (Figure 12). The correlation coefficient ($R^2$) (1.00) (Figure 13) indicates a good relationship between the parameters and shows that the pseudo-second-order model simulates the data better than the pseudo-first-order kinetic model. Based on these results shown in Table 2, the observation was made that the pseudo-second-order model simulate the data well.

## CONCLUSIONS

Based on the result of this study, the following conclusions were drawn olive leaves powder was prepared and tested for surface adsorption for crystal violet, and the results indicated amorphous nature suitable for adsorption of particulates. The olive leaves powder based on the maximum adsorption capacity has shown strong potential to capture crystal violet from solutions. The adsorption of crystal violet onto OLP increases with an increase in the initial concentration of adsorbate and time of contact until equilibrium, which achieves at 20 min. The maximum percentage adsorbed was obtained at pH of 7.5 and a minimum at pH 2. Equilibrium of adsorption was studied, and the result indicated that the Langmuir and Freundlich isotherm models best described the adsorption equilibrium. Kinetics study for the adsorption of crystal violet onto OLP was observed to follow the pseudo-second-order model. The research presented olive leaves powder as an effective, efficient, benign and cheap alternative biosorbent for the sequestration of dyes from solutions.

## ACKNOWLEDGEMENTS

We would like to acknowledge the Faculty of Arts and Science Msallata at Elmergib University for providing all facilities to complete this research.

## REFERENCES

Alkherraz, A.M., Ali, A.K., Elsherif, K.M., El-Dali, A., 2019. Biosorption Study of Zn(II), Cu(II), Pb(II) and Cd(II) ions by palm leaves activated carbon. Chemistry International 4, 8-17.

Alkherraz, A.M., Ali, A.K., Elsherif, K.M., El-Dali, A., 2020a. Removal of Pb(II), Zn(II), Cu(II) and Cd(II) from aqueous solutions by adsorption onto olive branches activated carbon: Equilibrium and thermodynamic studies. Chemistry International 6(1), 11-20.

Alkherraz, A.M., Ali, A.K., Elsherif, K.M., El-Dali, A. 2020b. Equilibrium and thermodynamic studies of Pb(II), Zn(II), Cu(II) and Cd(II) adsorption onto Mesembryanthemum activated carbon. Journal of Medicinal and Chemical Sciences 3(1), 1-10.

Araújo, F.V.F., Yokoyama, L., Teixeira, L.A.C., 2006. Color removal in reactive dye solutions by UV/$H_2O_2$ oxidation. Química Nova 29(1), 11-14.

Banerjee, S., Chattopadyaya, M.C., 2017. Adsorption characteristics for the removal of a toxic dye, tartrazine from aqueous solutions by a low cost agricultural by-product. Arabian Journal of Chemistry 10, S1629-S1638.

Betiku, E., Sheriff, O.A., 2014. Modeling and optimization of Thevetia peruviana (yellow oleander) oil biodiesel synthesis via *Musa paradisiacal* (plantain) peels as heterogeneous base catalyst: A case of artificial neural network vs. response surface methodology. Industrial Crops and Products 53, 314-322.

Caldeira, A.S., Fabris, J.D., Nelson, D.L., Damasceno, S.M., 2018. Removal of textile dye by adsorption on the cake as solid waste from the press-extraction of the macaúba (*Acrocomia aculeata*) kernel oil. Eclética Química Journal 43(1), 48-53.

Calvete, T., Lima, E.C., Cardoso, N.F., Vaghetti, J.C., Dias, S.L., Pavan, F.A., 2010. Application of carbon adsorbents prepared from Brazilian-pine fruit shell for the removal of reactive orange 16 from aqueous solution: kinetic, equilibrium, and thermodynamic studies. Journal of Environmental Management 91(8), 1695–1706.

Dada, A.O., Ojediran, J.O., Olalekan, A.P., 2013. Sorption of $Pb^{+2}$ from aqueous solution unto modified rice husk: isotherm studies. Advances in Chemical Physics 2013, 1-6.

Demirbas, A., 2004. Effects of temperature and particle size on bio-char yield from pyrolysis of agricultural residues. Journal of Analytical and Applied Pyrolysis 72(2), 243-248.

El-Hashani, A., Edbey, K., Elsherif, K.M., Alfaqih, F., Alomammy, M., Alomammy, S., 2018a. Biosorption of Eriochrome Black T (EBT) onto waste tea powder: equilibrium and kinetic studies. To Chemistry Journal 1(3), 263-275

El-Hashani, A., Elsherif, K.M., Ben Khayal, N., 2018b. Size selective transport of aromatic molecules across parchment paper treated with prussian blue. Chemical Methodologies 2(3), 197-206.

Elsherif, K.M., Yaghi, M.M., 2016. Studies with model membrane: determination of fixed charge density of

silver sulfite membrane. American Journal of Polymer Science and Technology 2(2), 28-33.

Elsherif, K.M., Yaghi, M.M., 2017a. Membrane potential studies of parchment supported silver oxalate membrane. Journal of Materials and Environmental Science 8(1), 356-363.

Elsherif, K.M., Yaghi, M.M., 2017b. Studies with model membrane: the effect of temperature on membrane potential. Moroccan Journal of Chemistry 5(1), 131-138

Elsherif, K.M., El-Hashani, A., El-Dali, A., 2014a. Bi-ionic potential studies for silver thiosulphate parchment-supported membrane. International Journal of Advanced Science and Technology 1(4), 638-646.

Elsherif, K.M., El-Hashani, A., Haider, I., 2018a. Biosorption of Fe(III) onto coffee and tea powder: Equilibrium and kinetic study. Asian Journal of Green Chemistry 2(4), 380-394.

Elsherif, K.M., El-Hashani, A., Haider, I., 2019. Biosorption of Co(II) ions from aqueous solution onto coffee and tea powder: Equilibrium and kinetic studies. Journal of Fundamental and Applied Sciences 11(1), 65-81.

Elsherif, K.M., El-Hashani, A., El-Dali, A., Musa, M., 2014b. Ion selectivity across parchment-supported silver chloride membrane in contact with multi-valent electrolytes. International Journal of Analytical and Bioanalytical Chemistry 4(2), 58-62.

Elsherif, K.M., El-Hashani, A., Haider, I., 2018b. Equilibrium and kinetic studies of Cu(II) biosorption onto waste tea and coffee powder (WTCP). Iranian Journal of Analytical Chemistry 5(2), 31-38

Elsherif, K.M., Ewlad-Ahmed, A.M., Treban, A., 2017a. Biosorption Studies of Fe(III), Cu(II), and Co(II) from aqueous solutions by olive leaves powder. Applied Journal of Environmental Engineering Science 3(4), 341-352

Elsherif, K.M., Ewlad-Ahmed, A.M., Treban, A., 2017b. Removal Of Fe(III), Cu(II), and Co(II) from aqueous solutions by orange peels powder: Equilibrium study. Biochemistry and Molecular Biology 2(6), 46-51

Fosso-Kankeu, E., Akinpelu, E.A., Keulder, M.Q., 2019. Banana peel as biosorbent for removal of brilliant green from aqueous solutions. 17th Johannesburg International Conference on Science, Engineering, Technology and Waste Management (SETWM-19). Nov. 18-19, 2019 Johannesburg, S. Africa.

Gupta, V.K., 2009. Application of low-cost adsorbents for dye removal-A review. Journal of Environmental Management 90, 2313-2342.

Gupta, V.K., Pathania, D., Kothiyal, N., Sharma, G., 2014. Polyaniline zirconium (IV) silicophosphate nanocomposite for remediation of methylene blue dye from waste water. Journal of Molecular Liquids 190, 139–145.

Mahmood, T., Aslam, M., Naeem, A., Sissique, T., Din, S., 2018. Adsorption of As(III) from aqueous solution onto iron impregnated used tea activated carbon: Equilibrium, kinetic and thermodynamic study. Journal of the Chilean Chemical Society 63, 3855-3866.

Nasuna, N., Hameed, B.H., Din, A.T.M., 2010. Rejected tea as a potential low-cost adsorbent for the removal of methylene blue. Journal of Hazardous Materials 175, 126.

Nworie, F.S., Nwabue, F.I., Oti, W., Mbam, E., Nwali, B.U., 2019. Removal of methylene blue from aqueous solution using activated rice husk biochar: Adsorption isotherms, kinetics and error analysis. Journal of the Chilean Chemical Society 64(1), 4365-4376.

Okareh, O.T., Adeolu, A.T., 2015. Removal of lead ion from industrial effluent using plantain (*Musa paradisiaca*) wastes. British Journal of Applied Science and Technology 8(3), 267-276.

Petrovic, M., Rarjenovic, J., Barceló, D., 2011. Advanced oxidation processes (AOPs) applied for wastewater and drinking water treatment. Elementation of pharmaceuticals. The Holistic Approach to Environment 1(2), 63-74.

Prakash, N.B., Sockan, V., Jayakaran, P., 2014. Waste water treatment by coagulation and flocculation. International Journal of Engineering Science and Innovative Technology 3(2), 479-484.

Reddy, C.A., Prashanthi, N., Babu, P.H., Mahale, J.S., 2015. Banana peel as a biosorbent in removal of nitrate from water. International Advanced Research Journal In Science, Engineering And Technology 2(10), 94-98.

Seid mohammadi, A., Asgari, G., Leili, M., Dargahi, A., Mobarakian, A., 2015. Effectiveness of Quercus branti activated carbon in removal of methylene blue from aqueous solutions. Archives of Hygiene Sciences 4 (4), 217–225.

Singh, J., Mishra, N.S., Banerjee, S.I., Sharma, Y.C., 2011. Comparative studies of physical characteristics of raw and modified sawdust for their use as adsorbents for removal of acid dye. BioResources 6, 2732.

Uchimiya, M., Chang, S., Klasson, K.T., 2011. Screening biochars for heavy metal retention in soil: Role of oxygen functional groups. Journal of Hazardous Materials 190(3), 432.

Zaidan, T., Salah, E., and Waheed, M., 2013. Banana peel as removal agent for sulfide from sulfur springs water. Civil and Environmental Research 3(10), 27-36.